Eur. Phys. J. D **20**, 347–355 (2002)
DOI: 10.1140/epjd/e2002-00171-6

THE EUROPEAN PHYSICAL JOURNAL D

Tautomer contributions to the near UV spectrum of guanine: towards a refined picture for the spectroscopy of purine molecules

W. Chin, M. Mons[a], I. Dimicoli, F. Piuzzi, B. Tardivel, and M. Elhanine

Laboratoire Francis Perrin[b], Service des Photons, Atomes et Molécules, Centre d'Études de Saclay, bâtiment 522, 91191 Gif-sur-Yvette Cedex, France

Received 24 June 2002
Published online 13 September 2002 –

Abstract. By using depopulation laser techniques, like IR-UV population labeling coupled to mass-selected R2PI detection, we confirm that four tautomers are responsible for the near UV spectroscopy (310–280 nm) of guanine: two enol and two keto forms, each pair having a 7NH and a 9NH form. Besides the UV spectroscopy of each tautomer, additional information on the excited state nature and dynamics is obtained from fluorescence studies. In particular, the quenching of fluorescence beyond 285 nm, the existence of a background absorption, as well as the existence of a strongly red-shifted component in the fluorescence emission provides evidence for a strong electronic mixing in the excited state together with an efficient non-radiative process. The details of these features are found to be tautomer-dependent. Comparison of the present results with literature data on other purine molecules, like adenine or 9-substituted guanines, enables us to propose a new insight on the spectroscopy and dynamics of the purine molecules. First, a large variability of the tautomer distribution in the gas phase is found within the purine family, in particular a molecular change, as simple as a 9-methylation on guanine, can reduce the tautomer distribution to a single species (enol form). Since the absorption spectrum is tautomer-dependent as well as substituent-dependent, it turns out that the tautomer population is one of the major parameters that control the overall shape of the UV spectrum. Second, the excited state model, often evoked in the literature, which involves electronic coupling between excited states of different natures, namely $\pi\pi^*$ and $n\pi^*$ states, might account for the present fluorescence measurements on guanine, providing an extensive excited state electronic mixing is assumed for these systems.

PACS. 33.20.Lg Ultraviolet spectra – 33.50.-j Fluorescence and phosphorescence; radiationless transitions, quenching (intersystem crossing, internal conversion) – 82.39.Pj Nucleic acids, DNA and RNA bases

1 Introduction

Gas phase studies of neutral biomolecules have known a huge development in the past decade [1]. Since the pioneering works on aminoacids, small peptides and pyrimidine bases [2–4], several experimental groups have focussed their studies either on the spectroscopy or the dynamics of these species [5–20]. The achievement of spectroscopic laser studies on these molecules now allows experimentalists to provide cutting edge spectral information, that theoreticians can use to validate their structural or spectral simulations.

Among the biomolecules studied in the gas phase, building blocks of the living world as nucleobases have received recently special attention from both experimentalists [6,9,10,12–15,17–20] and theoreticians [21–39]. DNA bases are indeed challenging species, for several reasons: first, their ability to exist as several forms (tautomers, see Fig. 1) due to the presence of labile H atoms on their skeleton; second, the complicated absorption spectrum due to both the presence of tautomers and a complex electronic structure, and the numerous π and n electrons and third, their fragile and thermolabile character that make difficult the running of gas phase experiments on it. In order to circumvent this last issue, desorption techniques have been developed in several groups and have led to a fast growing literature.

The gas phase purine DNA bases have been studied using state-of-the-art UV and IR laser spectroscopy. Adenine and 9-methylated adenine were recently investigated [10,12,17]. These supersonic expansion studies indicate that the near UV spectroscopy of adenine is quite poor, essentially characterised by four close lying bands, hardly consistent with a vibronic Franck-Condon activity, and exhibiting a weak fluorescence emission. The lifetime

[a] e-mail: mmons@cea.fr
[b] URA CEA-CNRS 2453

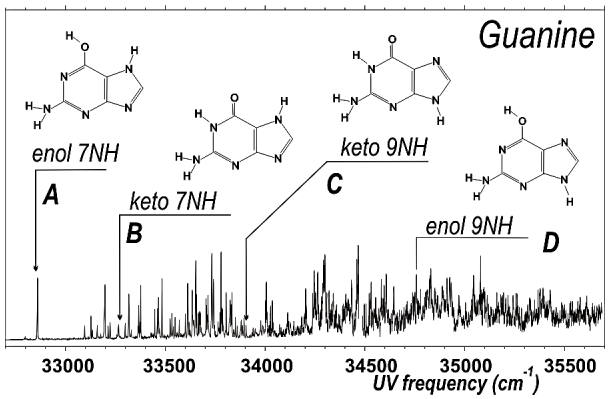

Fig. 1. Mass-selected one-color resonant two-photon ionisation spectrum of guanine in the near UV region (310–280 nm). Arrows indicate origin transitions of the four tautomers of guanine identified in a previous study (Ref. [20]) together with the corresponding assignment.

of the excited state on the most intense band was measured to be 8 ps. One group report that these main bands are also accompanied with more red and weak band system that do not appear in the fluorescence spectrum [10]. Besides this, the same authors also report the observation of a wide background that extends far to the blue. Pertubative and mixing electronic effects between a bright $\pi\pi^*$ singlet and a $n\pi^*$ singlet states lying in this spectral region have been invoked to account for the anomalous vibrational spacing, the short lifetime as well as the occurrence of the wide background absorption, however, without any direct proof for this involvement. In particular, although the assignment of four main bands to the same tautomer (the 6-amino 9NH form) was very recently established, the assignment of the red system in terms of tautomer remains an open question.

In a first attempt to rationalise the effect of substitutions on the purine aromatic system, de Vries and coworkers also investigated a series of purines, including guanine, 2-aminopurine (2AP), as well as a few 9 substituted purines [13]. The near UV spectra of guanine and 2-aminopurine are at odd with that of adenine. They turn out to be strongly red-shifted compared to adenine and to exhibit a rich Franck-Condon activity, extending far to the blue (typically at least 2 000 cm^{-1} above the origin). These authors interpreted the spectroscopic differences in terms of a much weaker (energy-controlled) interaction between the $\pi\pi^*$ and $n\pi^*$ excited singlet states in this case compared to adenine and attributed this to the effect of amino substitution in the position 2 of purine. Similarly, the 9-substituted purines studied all exhibit rather blue shifted spectra, characterised by short Franck-Condon activities, leading the authors to assign this behaviour to an electronic effect caused by the 9-substitution. Although the authors mention the possible existence of tautomers, especially for guanine, its effect on the overall shape of the spectra of other systems was not considered.

Concerning tautomerism, the case of guanine (Gua) turns out to be rather interesting and challenging. Several successive investigations brought pieces of information on the system, thus completing the puzzle one piece after the other. Nir *et al.* first provided evidence for the complexity of the near UV spectrum of guanine in their one-colour resonant two-photon ionisation (R2PI) experiment [6]. Piuzzi *et al.* showed the fluorescent nature of the excited state of at least two tautomers [15]. Then using IR-UV hole burning experiments, Nir *et al.* showed the existence of three forms and proposed an assignment in terms of tautomers, based on the relative stabilities as well as on a comparison between experimental and *ab initio* IR spectra [14]. Finally, choosing an alternative strategy based on a systematic search for tautomers, together with a systematic comparison of the IR/UV spectra between guanine and methylated guanines, our group proposed an overall consistent picture of the near UV absorption spectrum of guanine [20]. A fourth form was discovered in the blue part of the spectrum; the assignment of the four forms in the order of increasing origin transition energies (Fig. 1) is: A, enol 7NH; B, keto 7NH; C, keto 9NH and D enol, 9NH, showing that the 7 *vs.* 9 NH tautomerism controls the transition energy, the 9NH forms being shifted to higher energies. This study confirmed nicely what was suspected earlier by Eastman [40] and by Wilson and Callis [41] for the 7/9NH tautomerism of guanine and adenine from comparisons between absorption and fluorescence excitation spectra in solution.

Incidentally, our gas phase study also showed that the most stable tautomers (in the case of Gua, the 9NH keto and enol forms, according to calculations) are not necessarily the most populated in the supersonic expansion following desorption [20]. More preoccupying for the relevance of gas phase studies, the same study revealed that in the 9-methylated substituted guanine, the biologically relevant keto form was completely absent.

Having secured the identification of the four tautomers enables us to propose a tautomer-dependent investigation of the excited state dynamics of the guanine molecule. In this context, the fluorescence diagnostic appeared to us particularly appealing, since it allows us to provide valuable information on the excited state nature and its dynamics. Following our first fluorescence studies carried out close to the origin of the A red most species [15], we have pursued our investigation to the blue, having in mind the fluorescence properties of the four forms observed and the nature of their spectral contribution as well.

The aim of the present paper is initially to provide the spectral signature of the four conformers using the modern non-linear spectroscopic laser toolbox, including hole burning and population labeling spectroscopy using resonance enhanced two-photon ionisation (R2PI) or laser-induced fluorescence (LIF), together with a dynamical characterisation of their excited state as measured by dispersed fluorescence spectra and fluorescence decays. The results together with the comparison with other purine derivatives lead us to propose a model that emphasises the prominent role of (i) tautomer population in the near UV spectroscopy of these molecules and (ii) the electronic mixing in the excited states of these species.

2 Experimental methods

The experiments were performed on two experimental set-ups, both composed of two vacuum chambers. The first set-up was specially designed for high-resolution ionisation diagnostic and equipped with a reflectron time-of-flight mass spectrometer; the second one combines both fluorescence and ionisation diagnostics and is equipped with a linear time-of-flight mass spectrometer. In each case, the pulsed expansion takes place in the first chamber and is generated by a pulsed valve (General Valve Corp. nozzle – diameter ~ 300 μm) fitted with a laser desorption device, already described [42]. The desorbed molecules cooled and entrained in the argon expansion (2 to 6 bars) can be probed directly by a laser beam, about 1 cm downstream from the nozzle by detecting the laser-induced fluorescence emission, after being filtered in a wide band monochromator (resolution: 30 nm). They can also be allowed to enter the second chamber, after passing through a skimmer, where R2PI is carried out. In this case, the resulting ions are mass-analysed by the TOF spectrometer and detected using microchannel plates.

The molecules are excited and ionized by the frequency-doubled output of an excimer pumped (Lambda Physik EMG 201) dye laser (Lambda Physik FL 3002). The fluorescence excitation spectra (FES) or mass-selected resonant two-photon ionisation spectra were obtained by monitoring respectively the variations of the fluorescence or of the molecular ion signals as a function of the laser wavelength. Three dyes (Rhodamin B and 6G, Coumarin 540A) were used for covering the spectral range.

The use of pump-probe spectroscopic methods, enables several type of spectra to be measured:

- UV–UV depopulation spectroscopy, which enables to selectively discriminate the contribution of each form of a given molecule in the UV spectrum;
- resonant ion-dip infrared (RIDIR) spectroscopy, with a tunable infrared laser source as pump laser, which provides the ground state infrared spectrum of the UV probed species;
- IR-labeled R2PI spectra (population labeling, PL), which enables to selectively discriminate the contribution of each form according to their IR absorption.

All the pulsed events, pulsed valve aperture, desorption laser shot and diagnostic laser shot, were carefully synchronized using suitable electronics. The IR laser source is an optical parametric oscillator (OPO) built by Euroscan. The tunable IR light is generated by the interaction of a Nd:YAG fundamental beam (Brillant, Quantel Corp, 400 mJ) with a $LiNbO_3$ crystal. The IR wavelength (idler) is tuned by tilting the crystal as well as an intracavity Fabry-Perot etalon. The IR covers the 2.6 to 4 μm domain, with however a hole centred at 2.87 μm corresponding to a strong impurity absorption in the crystal. For desorption, we used the second harmonic of a Nd:YAG laser (Minilite-Continuum Corp.) with an energy density of the order of 0.5 J/cm^2, transported to the sample by an optical fiber. As a rule, the crystalline sample of molecules under study were reduced to powder, then mixed with graphite powder, as homogeneously as possible, and finally sintered under high pressure in order to obtain a solid disc (diameter 13 mm – thickness ~ 1.5 mm) which can be easily fixed very close to the valve orifice.

The dispersed fluorescence spectra were obtained by using a spectrometer (300 mm focal length – $f/4$ aperture – SP306i – Acton Research Corp.) equipped with a pulsed intensified 1024×056 CCD detector (PI-MAX-1024-RB Princeton Instruments – Roper Scientific). We used mostly the grating corresponding to the best resolution achievable, *i.e.* 600 grooves/mm (blazed at 500 nm). The detector sensitivity is constant between 200 and 550 nm. The value of the slit aperture was set in order to obtain a reasonable spectral resolution (10 μm slit corresponds to a resolution of 0.1 nm at 436 nm) together with a good signal-to-noise ratio for a reasonable number of laser shots. We used mostly a slit aperture of 0.5 mm corresponding to a resolution of ~ 100 cm^{-1}. Averaging over a number of 1 200 laser shots provided a good compromise between acquisition time and signal to noise ratio. The CCD intensifier was externally triggered and synchronized with the fluorescence emission. The intensification gate and gain were fixed to 50 ns and $\sim 10^7$ respectively. As a rule, when recording the dispersed spectrum corresponding to the excitation of a given absorption band, we subtracted the dispersed spectrum obtained when exciting the background absorption close to the band considered. This provided the mean of discriminating both the intrinsic detector noise and the spectral contribution from an eventual underlying background due to carbon species.

3 Experimental results

3.1 R2PI spectroscopy

Figures 1 and 2b show the spectrum of Guanine in the near UV as revealed by mass-selected one-colour R2PI spectroscopy. Also indicated in Figure 1 are the origin bands observed for the four tautomers (assigned to a $\pi\pi^*$ transition) and their corresponding assignment as obtained in our previous IR-UV measurements: 7NH enol at $32\,864 \pm 5$ cm^{-1}, 7NH keto at $+405$ cm^{-1}, 9NH keto at $+1\,046$ cm^{-1} and 9NH enol at $+1\,891$ cm^{-1} [20].

A species. The spectrum of Figure 1 is very rich. In the red-most region ($\nu < 34\,000$ cm^{-1}), due to A alone, one observes a dense series of sharp, well-resolved and intense bands, starting from a relatively intense origin band. Such a pattern suggests *a priori* a wide Franck-Condon envelop, which can be ascribed to a significant geometry change between the ground and the excited electronic states. Surprisingly, a high density of vibrational excitations is observed even in the low frequency region ($\nu \sim 33\,200$ cm^{-1}); a few weak bands are also found very close but below the origin of A; a former hole-burning work allowed us to conclude that these weak bands do belong to the same species A [15]. Looking closely beyond 34 000 cm^{-1} (Figs. 1 and 2b), one also notices a slowly increasing background. Concomitantly, the density

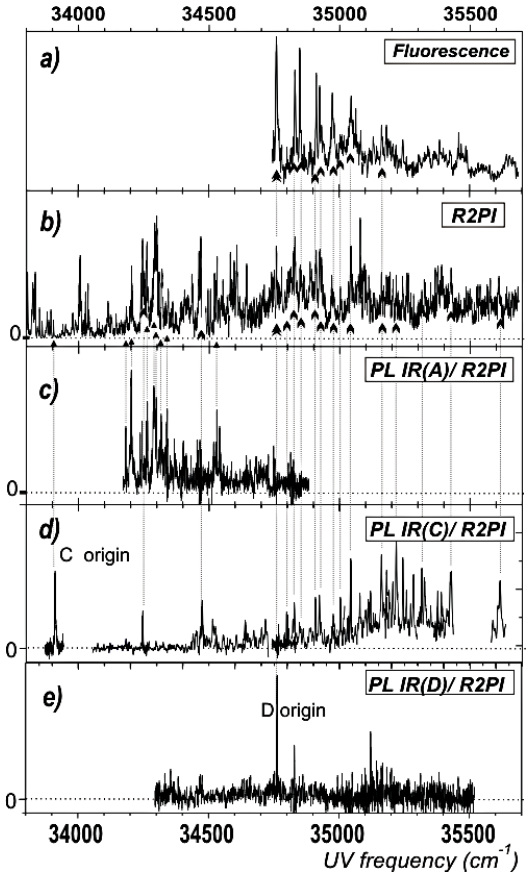

Fig. 2. UV spectroscopy of guanine in the 34 000–35 500 cm^{-1} spectral region: comparison between (a) the fluorescence excitation spectrum, (b) the mass resolved one-color R2PI spectrum and (c–e) the IR-R2PI population labeling spectra of species A, C and D, obtained with the IR laser tuned respectively on IR transitions at 3 577, 3 449 and 3 590 cm^{-1}. The population labeling spectra enable us to distinguish the individual contribution of tautomers to the R2PI and fluorescence spectra.

of bands seems also to increase together with their bandwidth. Since this region does also correspond to the onset of the UV spectrum of both the C and D 9NH species, we have performed population labeling spectra [20] of the A, C and D species in order to disentangle the several contributions in this range. In order to appreciate the contribution of the A species to the absorption spectrum in the 35 000 cm^{-1} region as well as to estimate the extension of its Franck-Condon envelop, a PL spectrum of A in this region has also been carried out (Fig. 2c). This spectrum clearly indicates a progressive disappearance of the discrete A features in this region (*i.e.* $\sim$ 1 700 cm^{-1} above the origin) together with their broadening and the existence of a significant background. This background, which starts *ca.* 1 200 cm^{-1} above the origin, is still present at 35 750 cm^{-1} (*i.e.* 2 800 cm^{-1} above the origin).

B species. The B species was discarded from the present study because of its too low intensity in our experiment. The UV-UV hole burning spectra of de Vries and co-workers [14] suggests a Franck-Condon activity similar to that of A for this tautomer, at least up to excitation energies as high as 600 cm^{-1}.

C species. Population labeling spectra (Figs. 2c–2e) show a large disparity between tautomers. The C spectrum (Fig. 2d) resembles that of A, close to the origin (Fig. 1), with narrow bands, organised in a pattern suggesting also a broad Franck-Condon envelop; discrete features are still observed at energies as high as 1 800 cm^{-1} above the origin, although they seem to become broad in this range. A slowly increasing background is observed, with an onset located *ca.* 1 000 cm^{-1} above the origin. This background is still present more than 2 000 cm^{-1} above the origin.

D species. The spectrum of the enol 9NH tautomer (Fig. 2e) seems to be qualitatively different from those of A and C, especially in the 500–600 cm^{-1} region from the origin, as testified by the present spectra (Figs. 1 and 2d). Although the PL spectrum has been extended compared to our previous study [20], only three significant bands were observed in the 34 300–35 500 cm^{-1} region. No signal was detected below the 34 755 cm^{-1} band, which we assign to the origin. In order to check that the absence of signal below 34 800 cm^{-1} is not due to a high ionisation energy for this species, a fluorescence excitation spectrum of guanine in this region was carried out (not shown). No evidence for additional significant bands due to the D species could be seen in this fluorescence spectrum.

This assignment is also corroborated by comparison with our data on 9-methyl guanine, whose assignment as an enol 9NH form has been firmly established from IR data by comparison with Gua D [20]. The UV spectrum of 9MeGua is very similar to that of Gua D, and is red shifted by only 143 cm^{-1} [20]. Neither the R2PI [13,20], nor the fluorescence excitation spectrum obtained by us (not shown) do exhibit any feature to the red of the main band, showing that this band is actually the origin. In addition, these findings also indicate that no trace of another tautomer (in particular of a keto form, expected to the red, according data on guanine) could be detected for this species in the gas phase.

From the comparison of spectra of Figures 1 and 2, it turns out that both A and C species are mainly responsible for the R2PI spectrum: A dominating the red part (ν < 34 500 cm^{-1}) and C the blue-most region. These species exhibit both discrete and continuous features. The formers are observed up to $\sim$ 1 700 cm^{-1} above the corresponding origin, which indicates spectrally extended FC envelopes. Simultaneously, backgrounds are also observed. The D species, on the other hand, does not fit in this scheme, with its much less extended spectroscopy as revealed by the PL spectra of Figure 2e and its absence of background.

3.2 Fluorescence excitation spectroscopy

Part of the fluorescence excitation spectrum of Gua in the 35 000 cm^{-1} region is shown (Fig. 2a) for the sake of comparison with the R2PI spectrum: all the lines found in

this spectrum do correspond to intense R2PI lines. The spectrum of Figure 2a, in which only the relatively long lifetime fluorescence signal ($\tau > 20$ ns) was recorded, provides evidence for excited state lifetimes in the ns time scale up to 35 200 cm^{-1}. Beyond this energy, fluorescence is quenched, in sharp contrast with the presence of discrete but broadened lines in both the R2PI and PL (C) spectra (Figs. 2b and 2d respectively). This discrepancy can be easily explained when one remarks that R2PI is able to detect ions even in the case of short-lived excited species, because the pumping-up rate to the ionisation continuum can be large enough to compete with the excited state non-radiative decay. This competition might also explain the relatively low intensity of the discrete bands due to C in this region (Fig. 2b).

3.3 Fluorescence decay times

Fluorescence decay times have been measured on the origin of the four tautomers, with the monochromator slits centred on the maximum of emission (*ca.* 320 nm). Off-resonance signals, taken in the wings of the bands, were subtracted in order to get rid of a possible background absorption contribution from carbone species. In all cases, decay times in the nanosecond range were found: 12, 22, 25 and 17 ± 2 ns for the origins of A, B, C and D respectively.

3.4 Dispersed fluorescence spectra

Dispersed fluorescence (DP) spectra have been recorded after excitation of several bands of guanine: the origin bands of A, B, C and D, as well as two bands of A and B in the region of the C origin and three bands of C in the region of the D origin (see Fig. 3). Like for temporal measurements, off-resonance signals were subtracted. A great care was taken with the help of light baffles to avoid detection of diffused laser light. The results displayed in Figure 3 show that two types of spectra are observed. First, spectra carried out on the origins of A, B and C (Figs. 3g, 3h and 3a, respectively), exhibit discrete features corresponding to the resonant fluorescence together with $\Delta v = 1$ transitions, which lead to the observation of clear vibrational discrete features up to 2 000 cm^{-1}, that seem to be superimposed on a broad red-shifted hump extending up to 7 000 cm^{-1} to the red. Second, broad featureless spectra, without discrete features but exhibiting the same red-shifted hump as in the first case, are observed in the A and C species for excited state energies above 700 cm^{-1} and as soon as the origin band of the D species (Fig. 3).

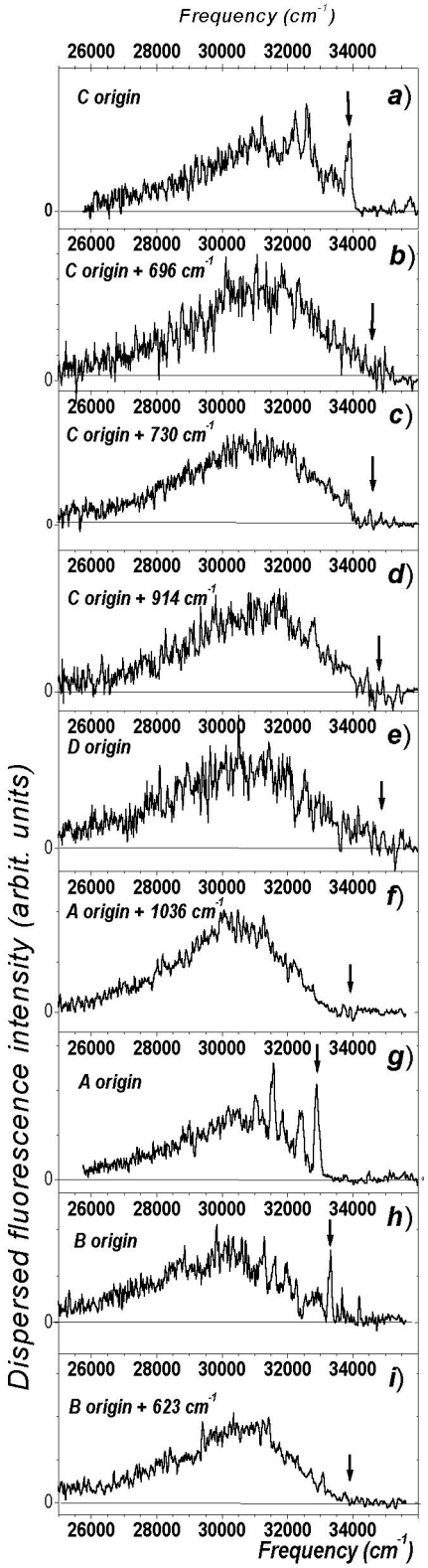

Fig. 3. Dispersed fluorescence spectra obtained after pumping several vibronic bands assigned, by RIDIR spectroscopy, to tautomers A (f–g), B (h–i), C (a–d) and D (e). In addition to the origin of each tautomer (g, h, a and e), spectra have also been recorded for intense bands in the region of the C (f and i) and D (b–d) origins. Only DF spectra on the A, B and C origins exhibit resonant fluorescence.

4 Interpretation and discussion

4.1 Tautomer population and relative stabilities

Four tautomers are observed in the gas phase for guanine. The question of experimental determination of

relative abundances is difficult to consider for several reasons. First, the oscillator strengths are probably tautomer-dependent, as suggested by Broo, who found a larger oscillator strength (by a factor of 3) for the lowest $\pi\pi^*$ transition of the enol 9NH form compared to 9NH keto [29]. Second, the origin bands are in separate spectral ranges, so that a precise relative intensity measurement is not easy to carry out. From the spectra alone, one can only conclude that the three A, C and D tautomers are probably present with comparable abundances. B is less populated in our experiment.

The most reliable theoretical data recently published on relative stabilities suggest that the two keto tautomers are the most stable forms, with comparable stability, then followed by the enol 9NH (higher by about 2 kcal/mol) and finally the enol 7NH (still higher by another 2 kcal/mol) [14,28]. This leads to the following ordering: B $\approx$ C $<$ D $<$ A.

The spectroscopic data, namely the origin transitions of each species, allows us to conclude about the relative stability in the excited state: B $<$ C $\approx$ A $\ll$ D. In particular, in the excited state D species (enol 9NH) is less stable than its keto counterpart C by more than 4 kcal/mol, and among the enol forms the stability order is reversed compared to the ground state.

4.2 Dependence of UV spectroscopy upon the tautomers

The present study provides evidence for a strong dependence of the near UV spectroscopic features upon the tautomer of guanine considered. The excitation spectrum of forms A and C (enol 7NH and keto 9NH) spans over more than 2 000 cm^{-1}, therefore suggesting a large distortion of the excited state relative to the neutral. Recent theoretical calculations support such a geometry change upon $\pi\pi^*$ excitation [38]. The case of D (enol 9NH) is apparently qualitatively different. Only a few bands are observed in this case; the origin being the most intense band. Although a similar distortion of the excited state relative to the ground state (and hence a similar FC envelop) is also expected [38], the absence of significant vibrational activity beyond 360 cm^{-1} suggests a very effective non-radiative process is at play in the excited state of this tautomer.

Obviously, despite their parentage, tautomers seem to have different photophysics, as different molecules would.

4.3 Nature and dynamics of the excited electronic states

4.3.1 Spectroscopy

All the tautomers of guanine are found to be fluorescent, at least on their origin band. The significant fluorescence signal corroborates the assignment of the transitions observed to a $\pi\pi^*$ transition. The nanosecond range fluorescence lifetimes measured is *a priori* in line with what is expected for a $\pi\pi^*$ transition, even if so far the nature of the fluorescent states still deserves discussion (see below). One can notice that the fluorescence decays measured on the origin bands for the enol species (A and D) are smaller than for the keto species (B and C), in qualitative agreement with the oscillator strength calculations for the first $\pi\pi^*$ transition by Broo and Holmén (assuming a negligible non-radiative decay) [26].

The surprising spectroscopic feature is the broad background absorption that starts 1 000–1 200 cm^{-1} above the origin of the $\pi\pi^*$ transition, and which is observed for both A and C species. The featureless spectrum suggests a fast excited-state dynamics, which is corroborated by the fluorescence observations. Indeed no long-lived ($\tau > 10$ ns) fluorescence is observed from the background. Unfortunately, no reliable information can be extracted about an eventual short-lived ($\lesssim$ 10 ns) guanine fluorescence, because, under the present experimental conditions, a short-lived background fluorescence from carbon clusters (formed from the graphite matrix) can also be observed.

4.3.2 Dynamics

Dispersed fluorescence data. The DF spectra obtained from the A, B and C origins are (at least partially) vibrationally resolved (Figs. 3g, 3h and 3a). A series of sharp features can be seen despite the modest spectral resolution of the experiment; the most intense and blue-most of which corresponds to the excitation energy (resonant emission from the initially excited level to the ground state vibrationless level). Superimposed to these structures is also seen a hump-shaped broad emission, which extends more than 7 000 cm^{-1} down to the red. The origin of this featureless structure deserves discussion. A first possible origin could be a dense series of vibrational bands, observed under low resolution. However, it should be noticed that in this case the broad Franck-Condon envelope, extending so far to the red, would not correspond to the mirror image of the absorption spectrum expected for emission. This suggests considering an alternative explanation. Such an interpretation can be proposed from other DF spectra obtained on vibronic bands of A, B and C (Figs. 3b–3d, 3f and 3i). In these cases, indeed, only featureless DF spectra are observed; the corresponding emission is red-shifted compared to the excitation and fits, in both shape and position, the hump-like broad emission detected on the DF spectra obtained on the origin bands.

All these data, combined to the different intensity ratios between sharp features and broad emission in the origin spectra of A, B and C, lead us to conclude to a dual nature for the fluorescence from the excited state and suggests that the excited state undergoes either vibrational or vibronic relaxation.

The first possibility that must be considered is the occurrence of intramolecular vibrational redistribution (IVR). In such a case, vibrational energy is expected to be, at least partially, redistributed among low frequency modes: emission takes place from a vibrationally relaxed species: the vibrational pattern is retained, although bands are broadened, and the blue-most band is

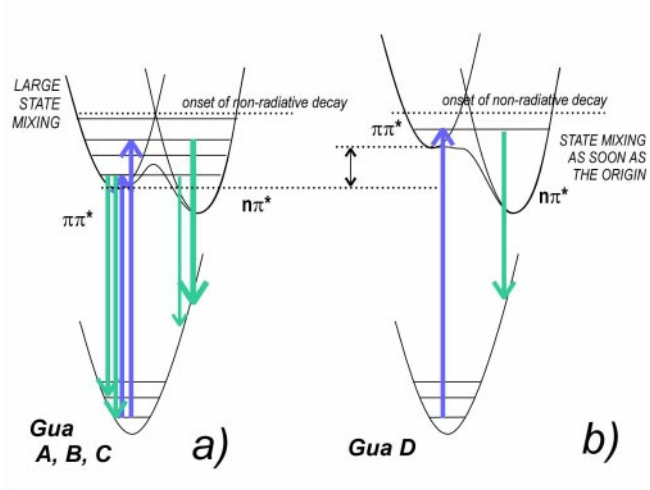

Fig. 4. Potential energy surface diagram and coupling model proposed to account for observations. (a) Case of A, B and C, showing a significant vibronic coupling as soon as the origin band, explaining a dual fluorescence feature on the origin. (b) Case of D, with a strong coupling on the origin, for instance due to a larger difference in the energetics of the electronic excited states involved, which account for the observation of a relaxed fluorescence.

located close to the transition origin, slightly red-shifted (shift < 200 cm^{-1}), because of the usually larger vibrational frequencies in the ground state compared to excited ones. Examples of this can be found in the literature, including in recent papers devoted to large molecules of biological interest [43,44]. From a careful examination of Figures 3b–3d, 3f and 3i, emission from the vibrationally excited species obviously do not fulfil these characteristics. In particular, no obvious hint of any resonant emission, even slightly red shifted, can be detected in the spectra.

A second possibility to account for the broad emission observed would be to consider excited state isomerisation between tautomers, which is, conceptually speaking, a generalised IVR process on a two-minima potential energy surface. The tautomerisation process that has the lowest barrier in guanine is probably the enol/keto process, compared to the 7/9NH interchange. Calculated ground state barriers are found to be of about 40 kcal/mol [28]. It seems to be doubtful that barriers would be as low as a few kcal/mol in the excited state of bare monomer.

We believe therefore that the discrete features of the emission spectra are due to the optically prepared vibrational levels of the excited electronic state, whereas the red-shifted emission should be ascribed to a vibronically relaxed but still fluorescent electronic manifold, populated *via* a strong vibronic mixing (Fig. 4).

This scenario is supported by the dynamical behaviour of the D tautomer (Fig. 3e), which does not exhibit any resonant emission, even on the origin transition. This forbids any purely vibrational relaxation process: either IVR or slow tautomerisation through a barrier. In some respect, this interpretation is reminiscent of that proposed to account for the emission of tryptophan compounds by Levy and co-workers [45,46], who assigned the fluorescence duality to an efficient electronic relaxation in the excited state.

Fluorescence quenching. A second striking result comes from the fluorescence quenching observed at excitation energies of the order of 1 500 cm^{-1} above the origin, with a small dependence upon the tautomer (A or C) considered. The lifetime of the excited state is therefore strongly lowered in these regions, in agreement with the apparent band broadening observed in the R2PI spectra. Fluorescence quenching is also observed for the D species, to a much larger extent, however, since no significant band is detected beyond 350 cm^{-1} above the origin, even in the R2PI population labeling experiment. These results provide evidence for the involvement of an efficient non-radiative process that considerably lowers the excited state lifetime in the high energy region.

4.4 Comparison with other systems and interpretation

According to the complexity of the band systems observed, it seemed to us legitimate to compare these results to those reported recently on other purine molecules, using the same investigation tools. In this line, recent studies on 2amino-purine [13] and adenine [10,12,13,17] appear quite interesting. A critical examination of the spectra suggests that these molecules seem to have spectroscopic features in common with guanine molecules:

- the presence of a broad absorption background, with the band series superimposed on it seems to be common in the purine photophysics: in particular, guanine A and C, adenine, 2-amino purine as well as dimethyl 2-amino purine seem to exhibit such a broad absorption;
- a large Franck-Condon activity is observed for guanine A, B, and C, 2-amino purine as well as dimethyl 2-amino purine, even if, in the two latter cases, part of the apparent vibronic activity might be assigned to other tautomers;
- a reduced Franck-Condon activity together with a fluorescence quenching is encountered with adenine, Gua D (enol 9NH), 9MeGua (enol). The 9-substituted guanines (ethylguanine, adenosine) studied by de Vries *et al.* [9,13] also show the same spectral behaviour: the spectra are all close to the Gua D spectrum, without significant FC activity, nor any trace of a keto tautomer, expected to the red, according to what is seen on guanine;
- weak bands, spectroscopically inconsistent with the intense band system, are observed for guanine A and adenine.

All these spectroscopic features together with the dynamic properties observed can be accounted for using a general photophysics model, like that recently evoked by Kim and co-workers [10] or de Vries and co-workers [13], which involves two interacting electronic states. If the state initially populated is probably a $\pi\pi^*$ state, as suggested by the intensity of the absorption spectra of purines

in the condensed phase, the nature of the second interacting state is less obvious. One possibility to consider is a $n\pi^*$ state, owing to the large number of n orbitals in guanine [10,13]. However, one should say that one has no direct proof for the involvement of a $n\pi^*$ state, even if excited states calculations situate roughly such a state in the region of the first $\pi\pi^*$ for all the purines [47], with however some specificity depending on the substituent considered.

Concerning the coupling, the mechanism could be seen as follows: the absorption from cold ground state is controlled by the $\pi\pi^*$ state that carries most of the oscillator strength. Coupling to the other manifold might occur through non-Born Oppenheimer vibronic coupling.

- On the origins of A, B and C, the dual DF can be understood in terms of a strong state mixing: the vibrationless level of the excited state is coupled to only one or only a few vibronic levels of the other manifold. In this case, (the so-called coarse distribution of interacting states, within the frame of the theory of non-radiative transitions [48,49]), the unperturbed (resonant) fluorescence of the $\pi\pi^*$ state should be observed. If the other manifold is also slightly fluorescent (in the case of a $n\pi^*$ state, because of Herzberg-Teller vibronic coupling, for instance), its fluorescence must also be observed. It can be expected broad and red-shifted according to the Franck-Condon principle between two electronic states of different natures (see Fig. 4a)). The vibronic coupling can also explain the weak bands observed in the vicinity of the origin band of A, which cannot be interpreted in terms of excitation of excited state totally-symmetric vibrational levels. Indeed, in such a case, $n\pi^*$ levels that cannot be populated from the ground state, can become partially allowed because of the electronic mixing.
- At higher excitation energies, the density of states in the second manifold can be so high that the coupling regime can switch to the "statistical limit" [48]. In this case, the large coupling to a dense manifold of vibronic states causes the irreversible non-radiative transition to occur: the resonant fluorescence is no longer observed to the benefit of a "relaxed" emission from the dense $n\pi^*$ manifold.
- At still higher density of vibronic states, the non-radiative transition theory [49] predicts Lorentzian line shapes to occur due to the fast non-radiative process populating the $n\pi^*$ state. This, combined to the large density of levels, might explain the occurrence of the background absorption observed in the spectra of A and C species.

Concerning the fluorescence, all our fluorescence excitation spectra and lifetime measurements were done with the monochromator mainly collecting the relaxed emission. The lifetime measurements therefore bring information on the non-radiative relaxation of the $n\pi^*$ manifold itself. Obviously, at vibrational excitations of the order of $1\,300\ \mathrm{cm}^{-1}$, it undergoes nanosecond time scale relaxation either *via* internal conversion or intersystem crossing; this latter process has indeed been shown to be at play as soon as on the origin band of A, since an ion signal was still observed in a two-colour R2PI experiment after a μs time scale delay by de Vries and co-workers [6].

Despite being different, the case of D (enol 9NH form) can be accounted for using the same theoretical framework, providing that an extended state mixing is already present as soon as the origin of the $\pi\pi^*$ transition. This can be simply explained by a lower energy of the $n\pi^*$ state with respect to the $\pi\pi^*$ state in this species (Fig. 4b), which is *a priori* favoured by the high energy of its $\pi\pi^*$ transition (D has indeed the blue-most origin among the four tautomers observed).

This model is also consistent with observations on other purine species:

- the 9NH tautomer of adenine exhibits the same dynamical trend as Gua D (scheme b of Fig. 4), with however a more efficient non-radiative decay. This would explain the weak fluorescence signal (low fluorescence quantum yield), the spectral perturbations as well as the occurrence of an absorption background, with weak broadened bands superimposed on it;
- more generally, a "A-type" behaviour seems to be observed for molecules exhibiting rather red spectra, like 2AP, whereas a "D-type" behaviour occurs for molecules presenting blue shifted spectra, like the 9NH tautomer of adenine. This confirms the trend observed on the guanine tautomers that the dynamical behaviour is controlled by the relative position of the $\pi\pi^*$ and $n\pi^*$ states.

5 Conclusions

General considerations on purine bases. The present results on guanine suggest that the near UV spectrum of a purine species can result from the spectral overlap of several tautomeric forms, each of them having its own photophysics, with proper excited state couplings, life times, etc. This study emphasises the fact that, although being very close in shape and electronic structure, tautomers should be considered as a set of individual species, even if their photophysics can probably be described by the same mechanism, with the energetics of the electronic states as a critical parameter.

Because of absorption spectra are found to be strongly tautomer-dependent as well as substituent-dependent, it turns out that the tautomer population is the major parameter that controls the overall shape of the UV spectrum. Therefore this conclusion forbids a general approach consisting in classifying the purine species according to the shape of their UV spectra, without distinguishing the tautomeric contributions.

A detailed understanding of the purine photophysics, and especially their dependence upon the nature of the substituent on the purine skeleton, requires to compare comparable data, namely data about the same type of tautomers (in particular 9NH and 7NH species should not be considered together). This is unfortunately not easy to carry out because the relevant information is often blurred by the dramatic variability of the tautomeric population

with the substituent. Among the most striking examples, let us notice that:

- adenine is only present as a 9NH tautomer in the gas phase [17], whereas both enol and keto forms of guanine exists under the 7 and 9NH forms;
- all the 9 substituted guanines are of enol type whereas both enol and keto forms are present in the 9NH tautomers of Gua, which leads to the conclusion that so far, the biologically relevant 9-substituted keto forms of guanine have not been observed in the gas phase.

In the same line, any experimental investigation of the puzzling issue of the very different photophysical behaviours (at least in solution) of the two purine isomers, 6AP (adenine, not fluorescent) and 2AP (strongly fluorescent), obviously requires the knowledge of the tautomer populations in the supersonic expansion. Indeed, the analogy with guanine suggests the strongly red shifted band system of 2AP might be due to a 7NH major tautomer; a second tautomeric form 9NH, if it exists, should therefore be looked for amid the rich vibronic system of the first tautomer, like are the B, C and D forms in the case of Gua. Such an hypothesis could be tested by comparing the 2AP spectrum with that of its methylated derivatives 7-methyl, 2-aminopurine and 9-methyl, 2-aminopurine, according to the successful strategy we applied previously for guanine [20]. In addition, detection and characterisation of the fluorescence of 2-aminopurine, the only purine that efficiently fluoresces in the condensed phase at room temperature, would also be another relevant test for the general validity of the models proposed.

References

1. E.G. Robertson, J.P. Simons, Phys. Chem. Chem. Phys. **3**, 1 (2001)
2. M.J. Tubergen, J.R. Cable, D.H. Levy, J. Chem. Phys. **92**, 51 (1990) and references therein
3. Y. Tsuchiya, T. Tamura, M. Fujii, M. Ito, J. Phys. Chem. **92**, 1760 (1988)
4. B.B. Brady, L.A. Peteanu, D.H. Levy, Chem. Phys. Lett. **147**, 538 (1988)
5. J.A. Dickinson, M.R. Hockridge, E.G. Robertson, J.P. Simons, J. Phys. Chem. A **103**, 6938 (1999)
6. E. Nir, L. Grace, B. Brauer, M.S. de Vries, J. Am. Chem. Soc. **121**, 4896 (1999)
7. C. Desfrançois, S. Carles, J.P. Schermann, Chem. Rev. **100**, 3943 (2000)
8. R. Weinkauf, F. Lehrer, E.W. Schlag, A. Metsala, Faraday Discuss. **115**, 363 (2000)
9. E. Nir, P. Imhof, K. Kleinermanns, M.S. de Vries, J. Am. Chem. Soc. **122**, 8091 (2000)
10. N.J. Kim, G. Jeong, Y.S. Kim, J. Sung, S.K. Kim, J. Chem. Phys. **113**, 10051 (2000)
11. E.G. Robertson, M.R. Hockridge, P.D. Jelfs, J.P. Simons, J. Phys. Chem. A **104**, 11714 (2000)
12. D.C. Lührs, J. Viallon, I. Fischer, Phys. Chem. Chem. Phys. **3**, 1827 (2001)
13. E. Nir, K. Kleinermanns, L. Grace, M.S. de Vries, J. Phys. Chem. A **105**, 5106 (2001)
14. E. Nir, C. Janzen, P. Imhof, K. Kleinermanns, M.S. de Vries, J. Chem. Phys. **115**, 4604 (2001)
15. F. Piuzzi, M. Mons, I. Dimicoli, B. Tardivel, Q. Zhao, Chem. Phys. **270**, 205 (2001)
16. T.S. Zwier, J. Phys. Chem. A **105**, 8827 (2001)
17. C. Plützer, E. Nir, M.S. de Vries, K. Kleinermanns, Phys. Chem. Chem. Phys. **3**, 5466 (2001)
18. E. Nir, C. Janzen, P. Imhof, K. Kleinermanns, M.S. de Vries, Phys. Chem. Chem. Phys. **4**, 740 (2002)
19. E. Nir, C. Janzen, P. Imhof, K. Kleinermanns, M.S. de Vries, Phys. Chem. Chem. Phys. **4**, 732 (2002)
20. M. Mons, I. Dimicoli, F. Piuzzi, B. Tardivel, M. Elhanine, J. Phys. Chem. A **106**, 5088 (2002)
21. I.R. Gould, N.A. Burton, R.J. Hall, I.H. Hillier, Theochem J. Mol. Struct. **331**, 147 (1995)
22. C. Colominas, F.J. Luque, M. Orozco, J. Am. Chem. Soc. **118**, 6811 (1996)
23. A. Broo, A. Holmén, Chem. Phys. **211**, 147 (1996)
24. J. Sponer, J. Leszczynski, P. Hobza, J. Biomol. Struct. Dyn. **14**, 117 (1996)
25. P. Hobza, J. Sponer, J. Leszczynski, J. Phys. Chem. B **101**, 8038 (1997)
26. A. Broo, A. Holmén, J. Phys. Chem. A **101**, 3589 (1997)
27. J. Leszczynski, J. Phys. Chem. A **102**, 2357 (1998)
28. L. Gorb, J. Leszczynski, J. Am. Chem. Soc. **120**, 5024 (1998)
29. A. Broo, J. Phys. Chem. A **102**, 526 (1998)
30. J.D. Gu, J. Leszczynski, J. Phys. Chem. A **103**, 2744 (1999)
31. T.K. Ha, H.-J. Keller, R. Gunde, H.-H. Gunthard, J. Phys. Chem. A **103**, 6612 (1999)
32. A.C. Borin, L. Serrano-Andres, M.P. Fulscher, B.O. Roos, J. Phys. Chem. A **103**, 1838 (1999)
33. O.V. Shishkin, L. Gorb, J. Leszczynski, Chem. Phys. Lett. **330**, 603 (2000)
34. S.X. Tian, K.Z. Xu, Chem. Phys. **264**, 187 (2001)
35. T.K. Ha, H.H. Gunthard, Spectroc. Acta Pt. A-Molec. Biomolec. Spectr. **57**, 55 (2001)
36. E.S. Kryachko, M.T. Nguyen, T. Zeegers-Huyskens, J. Phys. Chem. A **105**, 128 (2001)
37. N.U. Zhanpeisov, J. Leszczynski, Struct. Chem. **12**, 121 (2001)
38. B. Mennucci, A. Toniolo, J. Tomasi, J. Phys. Chem. A **105**, 7126 (2001)
39. B. Mennucci, A. Toniolo, J. Tomasi, J. Phys. Chem. A **105**, 4749 (2001)
40. J. Eastman, Ber. Bunsenges. Phys. Chem. **73**, 407 (1969)
41. R.W. Wilson, P.R. Callis, Photochem. Photobiol. **31**, 323 (1980)
42. F. Piuzzi, I. Dimicoli, M. Mons, B. Tardivel, Q. Zhao, Chem. Phys. Lett. **320**, 282 (2000)
43. W.L. Ryan, D.J. Gordon, D.H. Levy, J. Am. Chem. Soc. **124**, 6194 (2002)
44. W.L. Ryan, D. H. Levy, J. Am. Chem. Soc. **123**, 961 (2001)
45. T.R. Rizzo, Y.D. Park, D.H. Levy, J. Chem. Phys. **85**, 6945 (1986)
46. J.R. Cable, M.J. Tubergen, D.H. Levy, J. Am. Chem. Soc. **111**, 9032 (1989)
47. J. Lipinski, Spectroc. Acta Pt. A-Molec. Biomolec. Spectr. **45**, 557 (1989)
48. M. Bixon, J. Jortner, J. Chem. Phys. **50**, 4061 (1969)
49. M. Bixon, J. Jortner, J. Chem. Phys. **50**, 3284 (1969)